Kolmogorov-Arnold Networks/Transformers

Dimitrios Georgoulopoulos, **03120008**, Ioannis Karaparisis, **03120866**, Ioakeim El-Hattab Bistrogiannis, **03120058**, Panagiotis-Alexios Spanakis, **03400274**, Gregory Trakas, **03400274**

***Abstract*—**
***Index Terms*—**

I. Introduction

II. Related Work

A. Kolmogorov-Arnold Networks (KANs)

The Kolmogorov–Arnold representation theorem states, in simplified form, that any continuous, real-valued function of several variables can be represented as a superposition of continuous univariate functions combined through addition. This insight inspires Kolmogorov–Arnold Networks (KANs), which aim to approximate complex functions by leveraging learnable univariate activation functions along the network's edges [Liu et al.(2025)Liu, Wang, Vaidya, Ruehle, Halverson, Soljačić, Hou, and Tegmark].

In traditional multilayer perceptrons (MLPs), learning is achieved through a sequence of linear transformations followed by fixed pointwise nonlinearities (e.g., ReLU). KANs, by contrast, integrate flexible, spline-based activation functions into each edge of the network. These splines can be refined by increasing the number of knots, thus enhancing the function approximation in an adaptive manner. For example, the original Kolmogorov–Arnold representation naturally corresponds to a 2-layer KAN with a shape of $[n,\, 2n+1,\, 1]$, where all operations are differentiable and the network can be trained via back propagation.

A critical aspect of KAN implementation is the use of *residual activation functions*. In practice, the activation function $\phi(x)$ is defined as the sum of a fixed basis function and a trainable spline component:

$$\phi(x) = w_b\, b(x) + w_s\, \text{spline}(x).$$

Here, the basis function is typically chosen as the SiLU (sigmoid-weighted linear unit),

$$b(x) = \text{silu}(x) = \frac{x}{1+e^{-x}},$$

and the spline function is expressed as a linear combination of B-spline basis functions:

$$\text{spline}(x) = \sum_i c_i\, B_i(x),$$

with the coefficients c_i being learned during training. The trainable factors w_b and w_s further control the overall magnitude of the activation function.

Proper initialization is essential for stable training. Typically, the spline component is initialized near zero (using a small variance, e.g., $\sigma = 0.1$ for the B-spline coefficients), while w_b is initialized following standard methods such as Xavier initialization. Moreover, since B-splines are defined on bounded intervals yet activation values may exceed these bounds during training, the spline grids are updated dynamically based on the input activations to maintain approximation accuracy.

Although, in theory, a KAN layer for a network of depth L and constant width N (with splines of order k defined over G intervals) requires $\mathcal{O}(N^{2L}(G+k))$ parameters, KANs are typically designed with much smaller widths N than conventional MLPs. This design choice not only reduces the overall parameter count but also contributes to better generalization, as demonstrated in the original works.

In summary, Kolmogorov–Arnold Networks offer a principled and efficient alternative to traditional MLPs by directly learning an adaptive, spline-based decomposition of complex functions. This unified treatment of linear transformations and nonlinear activations yields lower test errors and improved interpretability, especially when modeling smooth or piecewise-smooth target functions.

III. Reproduction Results for Toy and Special Functions

In our reproduction study, we closely followed the experimental setup and evaluation criteria described in the original KAN work. Our experiments were divided into two parts: one focusing on toy functions with known smooth Kolmogorov–Arnold (KA) representations, and the other on a collection of challenging multivariate special functions.

A. Toy Functions

For the toy function experiments, we considered several target functions including:

- The univariate Bessel function: $f(x) = J_0(20x)$,
- A bivariate function: $f(x_1, x_2) = \exp\big(\sin(\pi x_1) + x_2^2\big)$,
- And additional simple functions such as $f(x_1, x_2) = x_1 x_2$.

Both Kolmogorov–Arnold Networks (KANs) and Multilayer Perceptrons (MLPs) were trained using the LBFGS optimizer over approximately 1800 steps. For the KANs, training was performed in refinement stages—starting with a coarse grid (with $G = 3$ knots) and increasing the number of knots up to 1000. At each refinement stage, an MLP with roughly the same number of parameters was designed as a baseline. The evaluation focused on tracking the train and test RMSE as a function of the model parameter count.

Figure 1 shows sample reproduction results for the Bessel function $f(x) = J_0(20x)$, while Figures 2 and 3 present results for the bivariate function $f(x_1, x_2) = \exp\big(\sin(\pi x_1) + x_2^2\big)$. In each case, the left panels depict the evolution of train and test losses versus training steps, and the right panels plot the final error as a function of the number of parameters.

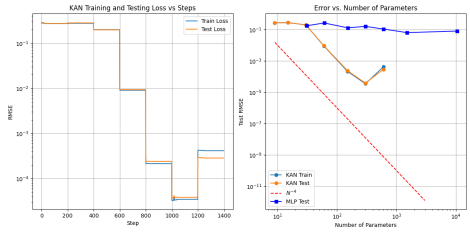

Fig. 1: Example: KAN vs. MLP for $f(x) = J_0(20x)$. (Left) Train/Test loss vs. steps; (Right) Error vs. #params.

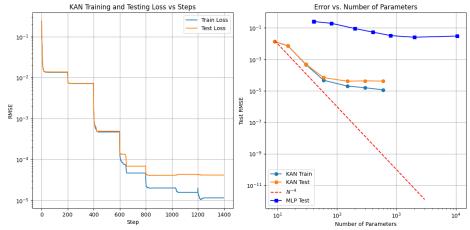

Fig. 2: Example: KAN vs. MLP on $f(x_1, x_2) = \exp\big(\sin(\pi x_1) + x_2^2\big)$. (Left) Train/Test loss vs. steps; (Right) Error vs. #params.

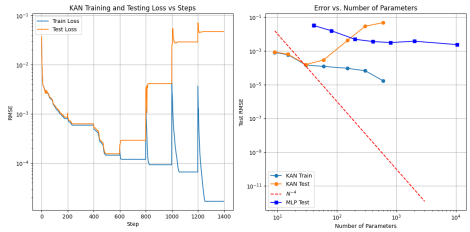

Fig. 3: Additional example for $f(x_1, x_2) = \exp\big(\sin(\pi x_1) + x_2^2\big)$. (Left) Train/Test loss vs. steps; (Right) Error vs. #params.

Our reproduction results on toy functions reveal that KANs exhibit abrupt reductions in test error immediately following an increase in the number of knots, whereas MLPs display more incremental improvements as additional hidden layers or units are added. Moreover, the learned univariate edge functions in KANs are particularly effective at approximating well-behaved smooth functions, thereby achieving lower RMSE with a comparable or even smaller parameter count.

B. Special Functions

We further extended our experiments to a diverse set of special functions that are common in mathematics and physics. These include incomplete elliptic integrals—both `ellipeinc` and `ellipkinc`—which often exhibit steep local changes or near-singular behavior for specific parameter combinations; associated Legendre functions such as `lpmv_m_1` and `lpmv_m_0`, whose polynomial-like structures can have large derivatives near the boundaries; and spherical harmonics, for example, `sph_harm_m_0_n_2`, which involves multiple local maxima and minima over angular coordinates.

Figure 4 illustrates sample results for the incomplete elliptic integral `ellipeinc` and the associated Legendre function `lpmv_m_1`. In addition, Figure 5 shows the reproduction result for the spherical harmonic `sph_harm_m_0_n_2`. In each case, the experiments confirm that KANs effectively capture the localized oscillatory and singular behavior of these functions.

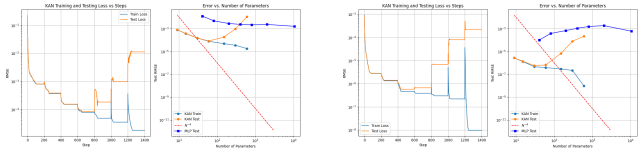

(a) `ellipeinc` (b) `lpmv_m_1`

Fig. 4: Sample results for special functions: (a) Incomplete Elliptic Integral (`ellipeinc`) and (b) Associated Legendre Function (`lpmv_m_1`).

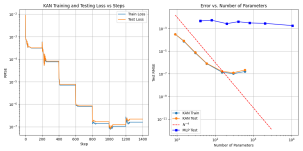

Fig. 5: Reproduction result for the spherical harmonic function `sph_harm_m_0_n_2`.

The key observations for special functions are that KANs partition the domain effectively and capture localized singularities or oscillatory behavior more adeptly than MLPs, and that although increasing the number of knots reduces training error, extreme refinement can sometimes lead to a slight increase in test error due to overfitting, particularly when the training dataset is limited. Furthermore, the Pareto frontiers, plotted in the RMSE versus parameter count plane, consistently demonstrate that KANs achieve lower error levels with fewer parameters compared to MLPs.

Overall, our reproduction experiments validate the original findings that KANs outperform traditional MLPs on both toy and special function approximation tasks. The adaptive refinement strategy in KANs allows for rapid error reduction and superior scaling with the number of parameters, while also offering interpretable, compact representations. These advantages make KANs a promising alternative for function approximation in various high-dimensional and challenging settings.

IV. KAT Finetuning on Image Datasets

In this section, we describe our finetuning procedure for adapting a pretrained KAT (ViT-based) model to various image recognition tasks. Our approach leverages the pretrained backbone from ImageNet [Deng et al.(2009)Deng, Dong, Socher, Li, Li, and Fei-Fei] and adapts the classification head to the target dataset, following a consistent data preprocessing and training strategy. In addition, we make use of GPU parallelism to accelerate training, taking advantage of multiple GPUs via PyTorch's `DataParallel` module.

Due to the limited capabilities of our training equipment (2 NVIDIA T4 GPUs), we utilized the smallest available pretrained model, which contains only 5.7 million parameters [Xingyi Yang(2025)]. This choice ensured that the model could be trained on the available hardware without running out of memory and helped reduce training time, allowing us to run multiple experiments. Consequently, we finetuned the model for only 5–10 epochs and employed early stopping to prevent overfitting.

A. Overall Finetuning Strategy

For each dataset (MNIST, FashionMNIST, CIFAR-10, and CIFAR-100), our finetuning procedure follows a consistent pipeline. First, we load a KAT model that has been pretrained on a large-scale dataset (ImageNet) to leverage its learned feature representations. In our case, due to limited hardware resources, we opted for the smallest pretrained model available (5.7M parameters) [Xingyi Yang(2025)]. Next, we adapt the classifier by resetting the classification head so that the output dimension matches the number of categories in the target dataset. In terms of data preprocessing, all images are resized to 224×224; for datasets with grayscale images, we replicate the single channel to form a 3-channel input, and we normalize the images using ImageNet statistics, namely, $\mu = [0.485, 0.456, 0.406]$ and $\sigma = [0.229, 0.224, 0.225]$.

During the training loop, we optimize the model using the AdamW optimizer. Importantly, we assign a lower learning rate to the pretrained backbone and a higher learning rate to the newly initialized classification head (about 10 times larger from $\approx 1e^{-5}$ to $1e^{-4}$). This strategy is adopted because the backbone is already pretrained on a large dataset and contains valuable, general features that we wish to preserve, whereas the classifier is randomly initialized and needs to learn quickly to adapt to the target domain. By using a tenth of the learning rate for the backbone, we minimize the risk of disrupting its learned representations while allowing the head to update more aggressively. Additionally, early stopping is employed to save the best checkpoint based on validation loss improvements.

Finally, we assess the model's performance by evaluating test set accuracy, generating confusion matrices, and plotting training and validation loss curves along with detailed classification reports. To further accelerate training, we leverage GPU parallelism by automatically wrapping the model using PyTorch's `DataParallel` module when multiple GPUs are available, ensuring efficient utilization of the hardware.

B. MNIST Finetuning Results

MNIST consists of handwritten digits (10 classes) in grayscale with an original size of 28×28 [Deng(2012)]. Images are upsampled to 224×224 and converted to 3 channels.

The finetuning process was run for 5 epochs with the learning rate for the classification head set to 1×10^{-5} and the backbone's learning rate set to one-tenth of that value. This configuration resulted in a final test accuracy of approximately 99.00%.

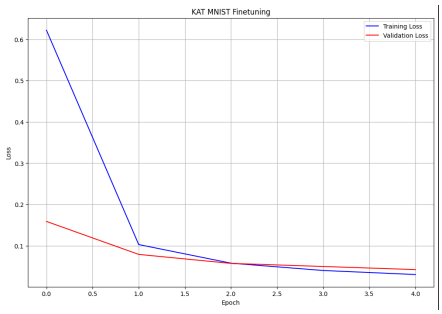

Fig. 6: MNIST: Training (blue) vs. Validation (red) Loss.

Class	Precision	Recall	F1-score	Support
0	0.99	1.00	0.99	980
1	0.99	1.00	1.00	1135
2	0.98	1.00	0.99	1032
...	...	...	...	...
8	0.99	0.99	0.99	974
9	0.99	0.98	0.98	1009
Accuracy		99.00%		

TABLE I: MNIST Classification Report (partial).

C. FashionMNIST Finetuning Results

FashionMNIST contains grayscale images of clothing items (10 classes) with an original size of 28×28 [Xiao et al.(2017)Xiao, Rasul, and Vollgraf]. The same preprocessing as MNIST is applied.

Finetuning was also performed for 5 epochs using the AdamW optimizer in conjunction with an early stopping mechanism, ultimately achieving a final test accuracy of around 92.78%.

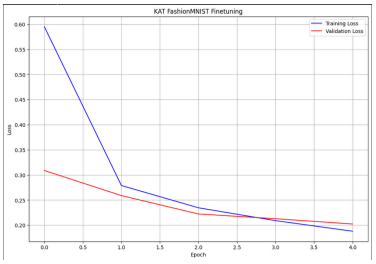

Fig. 7: FashionMNIST: Training vs. Validation Loss over 5 epochs.

Class	Precision	Recall	F1-score	Support
0 (T-shirt/Top)	0.90	0.85	0.87	1000
1 (Trouser)	0.99	0.99	0.99	1000
2 (Pullover)	0.93	0.87	0.90	1000
3 (Dress)	0.91	0.92	0.92	1000
4 (Coat)	0.89	0.93	0.91	1000
5 (Sandal)	0.99	0.98	0.99	1000
6 (Shirt)	0.75	0.82	0.79	1000
7 (Sneaker)	0.98	0.95	0.96	1000
8 (Bag)	0.99	0.99	0.99	1000
9 (Ankle Boot)	0.95	0.98	0.97	1000
Accuracy		93.01%		

TABLE II: FashionMNIST Classification Report.

D. CIFAR-10 Finetuning Results

CIFAR-10 consists of 10 classes of color images (originally 32×32) which are resized to 224×224 [Krizhevsky(2009)]. Preprocessing involves normalization with ImageNet statistics.

Similarly, for CIFAR-100, the model was finetuned over 5 epochs with early stopping—where the best validation loss was recorded at epoch 5—and a final test accuracy of approximately 95.70% was obtained.

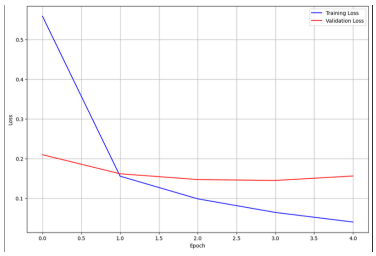

Fig. 8: CIFAR-10: Training vs. Validation Loss.

Class	Precision	Recall	F1-score	Support
0 (Airplane)	0.98	0.95	0.97	1000
1 (Automobile)	0.97	0.98	0.97	1000
2 (Bird)	0.98	0.95	0.97	1000
...	...	...	...	...
8 (Ship)	0.96	0.99	0.98	1000
9 (Truck)	0.97	0.96	0.97	1000
Accuracy		95.70%		

TABLE III: CIFAR-10 Classification Report (partial).

E. CIFAR-100 Finetuning Results

CIFAR-100 features 100 classes of color images (originally 32×32) [Krizhevsky(2009)] and is similarly preprocessed by resizing to 224×224 and normalizing with ImageNet statistics.

Similarly, for CIFAR-100, the model was finetuned over 5 epochs with early stopping—where the best validation loss was recorded at epoch 5—and a final test accuracy of approximately 81.17% was obtained.

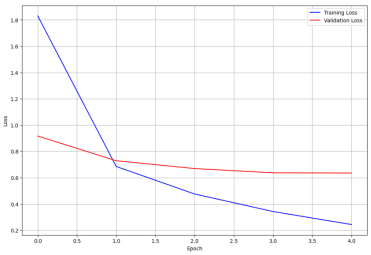

Fig. 9: CIFAR-100: Training vs. Validation Loss.

Class	Precision	Recall	F1-score	Support
Class 0	0.90	0.97	0.93	1000
Class 13	0.80	0.81	0.81	1000
Class 35	0.48	0.62	0.54	1000
...	...	...	...	...
Weighted Avg	0.82	0.81	0.81	10000

TABLE IV: CIFAR-100 Classification Report (excerpt).

F. Summary of Finetuning Results

Across all datasets, the finetuning procedure demonstrates that the pretrained KAT model adapts efficiently to new tasks. Specifically, we achieved test accuracies of approximately 99.00% on MNIST, 93.01% on FashionMNIST, 95.70% on CIFAR-10, and 81.17% on CIFAR-100. These results highlight the versatility of the KAT architecture, which effectively leverages large-scale pretrained features and GPU parallelism to achieve strong performance on diverse image recognition tasks within a short finetuning period. Moreover, the KAT model effectively and efficiently retains the previously learned knowledge from pretraining, adjusting quickly and properly to new information. Overall, our results demonstrate the potential of KAT models for image recognition tasks and the benefits of leveraging such pretrained models for efficient transfer learning.

REFERENCES

[Deng et al.(2009)Deng, Dong, Socher, Li, Li, and Fei-Fei] Jia Deng, Wei Dong, Richard Socher, Li-Jia Li, Kai Li, and Li Fei-Fei. Imagenet: A large-scale hierarchical image database. In *2009 IEEE Conference on Computer Vision and Pattern Recognition*, pages 248–255, 2009. doi: 10.1109/CVPR.2009.5206848.

[Deng(2012)] Li Deng. The mnist database of handwritten digit images for machine learning research [best of the web]. *IEEE Signal Processing Magazine*, 29(6):141–142, 2012. doi: 10.1109/MSP.2012.2211477.

[Krizhevsky(2009)] Alex Krizhevsky. Learning multiple layers of features from tiny images. 2009. URL https://api.semanticscholar.org/CorpusID:18268744.

[Liu et al.(2025)Liu, Wang, Vaidya, Ruehle, Halverson, Soljačić, Hou, and Tegmark] Ziming Liu, Yixuan Wang, Sachin Vaidya, Fabian Ruehle, James Halverson, Marin Soljačić, Thomas Y. Hou, and Max Tegmark. Kan: Kolmogorov-arnold networks, 2025. URL https://arxiv.org/abs/2404.19756.

[Xiao et al.(2017)Xiao, Rasul, and Vollgraf] Han Xiao, Kashif Rasul, and Roland Vollgraf. Fashion-mnist: a novel image dataset for benchmarking machine learning algorithms, 2017. URL https://arxiv.org/abs/1708.07747.

[Xingyi Yang(2025)] Xinchao Wang Xingyi Yang. Kolmogorov-arnold transformer. In *The Thirteenth International Conference on Learning Representations*, 2025. URL https://openreview.net/forum?id=BCeock53nt.